Colloid Polym Sci (2015) 293:975–983
DOI 10.1007/s00396-014-3480-9

SHORT COMMUNICATION

Self-assembly of 12-hydroxystearic acid molecular gels in mixed solvent systems rationalized using Hansen solubility parameters

C. Liu · M. Corradini · M. A. Rogers

Received: 9 October 2014 / Revised: 27 November 2014 / Accepted: 30 November 2014 / Published online: 11 December 2014

Abstract Recent advances in understanding the underlying mechanisms of self-assembly in molecular gels using Hansen solubility parameters (HSPs) have focused on gelator-single solvent mixtures. Linear correlations between critical gelator concentration (CGC) and polar HSP formed in specific regions where each region has the same proportion of octane with different ratios of either 1-octanol and 1-octylamine. CGC increases with an increasing proportion of 1-octanol and a decreasing proportion of 1-octylamine as the polar HSP increases within each region. Both G′ and breaking points decrease in a log-linear fashion as each individual HSP or total HSP increases, suggesting that 1-octanol-rich gels do not form strong gels because of hydrogen bonding between 1-octanol and 12HSA which is capable of impeding fiber growth. The interaction between 12HSA and 1-octanol is more disruptive to fiber growth than 1-octylamine which arises because of the solvents ability to accept or donate a hydrogen bond.

Keywords Molecular gels · Hansen solubility parameters · Critical gelator concentration · Low molecular weight organogelators · Self-assembled fribrillar network

Introduction

Molecular gels, comprised of low molecular weight organogelators (LMOGs), are thermally-reversible, semi-solid materials where the solvent is immobilized on a macroscopic scale by the three-dimensional (3D) self-assembled fibrillar network (SAFiN) [1–3]. LMOGs aggregate onto the SAFiN by physical, non-covalent interactions including hydrogen bonding, [4–7] pi-pi stacking, [8] dipole-dipole interactions, [9, 10] and London dispersion forces. [11] A precise balance between gelator-gelator interactions and gelator-solvent interactions is required for SAFiN formation; excessive gelator-gelator interactions interfere with unidirectional fibrillar growth leading to thicker fibers and eventually impede fibrous structures from forming. [12, 13] LMOGs have become a major topic of interest over the past decade because of their wide range of potential applications pertaining to photovoltaics, [14] light harvesting, [15] controlled drug release, [16] and *trans* and saturated fat replacement. [17].

The capacity of LMOGs to result in SAFiNs, and ultimately molecular gels, has been widely studied. [18–20] Numerous attempts to correlate solvent parameters to gelation have been meet with mixed success. Bielejewski et al. showed that the hydrogen-bonding network of 1,2-*O*-(1-ethylpropylidene)-α-D-glucofuranose and their thermal stability were both affected by solvent polarity. [21] Later, solvent chemistry was tailored using ethanol as a co-solvent with toluene to control polarity and hydrogen-bonding interactions of diphenylalanine (L-Phe-L-Phe, FF). [22] Of the solvent parameters studied, Hansen solubility parameters (HSPs), which consists of dispersive interactions (δ_d), polar interactions (δ_p), and hydrogen-bonding interactions (δ_h), have been the most useful at predicting 12HSA gelation ability and it appears that δ_h correlates most strongly with gelation ability and solvent chemistry [1, 13, 18, 23–29]. It is has been shown that the δ_h has a positive linear correlation with critical gelation concentration (CGC) for 12HSA [12, 13].

The majority of research with regards to HSPs and molecule gels has focused on a gelator mixed in a single solvent. To date, only a handful of studies have been completed on a mixed dual solvent systems using HSPs [27, 30–33] One such study included the properties of Pyrenyl-Linker-Glucono gelators in tetrahydrofuran-water mixtures were examined

C. Liu · M. Corradini · M. A. Rogers (✉)
School of Environmental and Biological Sciences, Department of Food Science, Rutgers University; The State University of New Jersey, New Brunswick, NJ 08901, USA
e-mail: rogers@aesop.rutgers.edu

[30]. They found the composition of the liquid mixtures had an effect on the solubility, gelation ability, crystallite size, CGC, microstructure, thermal, and mechanical stabilities of the gels, etc. [30]. The likelihood of gel formation depends on the HSPs of gelator and solvent combinations; the rheological properties of the gel illustrate the importance of the hydrogen-bonding interactions and mechanical stability [30]. Strong correlations found between δ_h and gel formation, for 12HSA, where $\delta_h < 4.7$ MPa$^{1/2}$ forms a clear gel, $4.7 < \delta_h < 6.5$ MPa$^{1/2}$ results in opaque gels or precipitate gels, and when $\delta_h > 6.5$ MPa$^{1/2}$, it remains a solution [13]. The hydrogen-bonding HSP seems to be a more predictive parameter than other solvent polarity measures for determining gelation behaviors for 1,3:2,4-dibenzylidene sorbitol (DBS) [34].

12HSA molecular gels have two different polymorphic forms depending on the solvent employed to make the gel: hexagonal subcells (~4.1 A) in non-polar (alkanes and thiols) and triclinic parallel subcells (~4.6, 3.9, and 3.8 A) in polar solvents (nitriles, aldehydes, and ketones) [24]. The hexagonal polymorphic form corresponded to the SAFiN with CGC less than 1 wt%. The triclinic polymorphic form corresponds to a less effective spherulitic supramolecular crystalline network and a corresponding CGC greater than 1.5 wt% [24]. In this study, the effect of ternary solvent mixtures using octane, 1-octanol, and 1-octylamine were employed at different ratios to investigate the effects on structure, thermal, and rheological properties of a 12HSA/solvent blend.

Methods

Materials and gel preparation

Octane, 1-octanol, 1-octylamine, and 12HSA were obtained from Sigma-Aldrich (St. Louis, MO) with purities greater than 0.95 % and were used without further purification. The solvents were selected because 12HSA in octane, forms a transparent gel, in 1-octylamine 12HSA forms an opaque gel or a precipitate gel and 12HSA in 1-octanol remains a solution at concentrations as high as 5 wt% [1, 13, 24, 25]. Using a ternary phase diagram, and varying the solvent ratio in 10 % increments, generated 66 solvent combinations. Initially, 1-g sample with 3 wt% 12HSA/solvent was prepared in 8 ml vials. Samples were heated to 100°C for 20 min and stored for 24 h at 25°C . The tube inversion method was used to determine if it was a gel; upon inverting the vial for 1 h if no flow was observed under its own weight, then the sample was classified crudely as a gel. If no flow was observed, the sample was diluted in by 0.5 %, reheated to 100 °C and cooled to 25°C , and re-tested until flow was observed; the last concentration that impeded flow was noted to be the CGC.

Polarized light microscopy

Polarized light micrographs were obtained for each 3 wt% 12HSA gels in each of the 66 solvent combinations using a Linkham imaging station (Linkham, Surrey, England) equipped with a Q imaging 2560× 1920 pixel CCD camera (Micropublisher, Surrey, Canada) and a 10× Olympus lens (0.25 NA) (Olympus, Tokyo, Japan). Samples were placed on a glass slide and covered by a glass coverslip. All the samples were observed at ~25°C under polarized light.

Rheological measurements

A discovery hybrid rheometer (TA instruments, New Castle, DE) was used to assess the rheological properties of the gels using an 80-mm flat peltier plate (TA instruments, New Castle, DE). An oscillatory stress sweep at 1 Hz was conducted between 0 and 5000 Pa to determine the linear viscoelastic region (LVR). Samples were prepared in aluminum molds comprised of Swagelok compression fittings, which acted as gas-tight seals to prevent the volatilization of the solvent during heating. The gels, obtained from the aluminum molds were 8 mm in diameter and 5 mm thick. The yield stress was determined when the G′ decreased from the LVR by 10 %.

Differential scanning calorimetry

Differential scanning calorimetry (DSC) (Q2000, TA Instruments, New Castle, DE) was used to determine the melting point of 6 to 10-mg sample sealed in hermetic aluminum pans (TA Instruments, New Castle, DE). The DSC chamber was maintained at 20°C and flushed with nitrogen (0.5 ml/min). The sample was then heated to 100°C at 2°C /min.

Results and discussion

Individual HSPs for the solvent combination are calculated using their weight percent distribution:

$$\delta_x = \sum (\delta_x)_i \varphi_i \quad (1)$$

where x stands for the dispersive, polar, or hydrogen-bonding component of i solvent where i represents octane, 1-octanol, or 1-octylamine. φ_i is the weight percent of component i in each mixture [35]. The HSP of 12HSA have previously been calculated using the group contribution method [36–39]. Hansen space was used to observe if the different states (i.e., sol, gel, or precipitate) of the 3 wt% 12HSA/

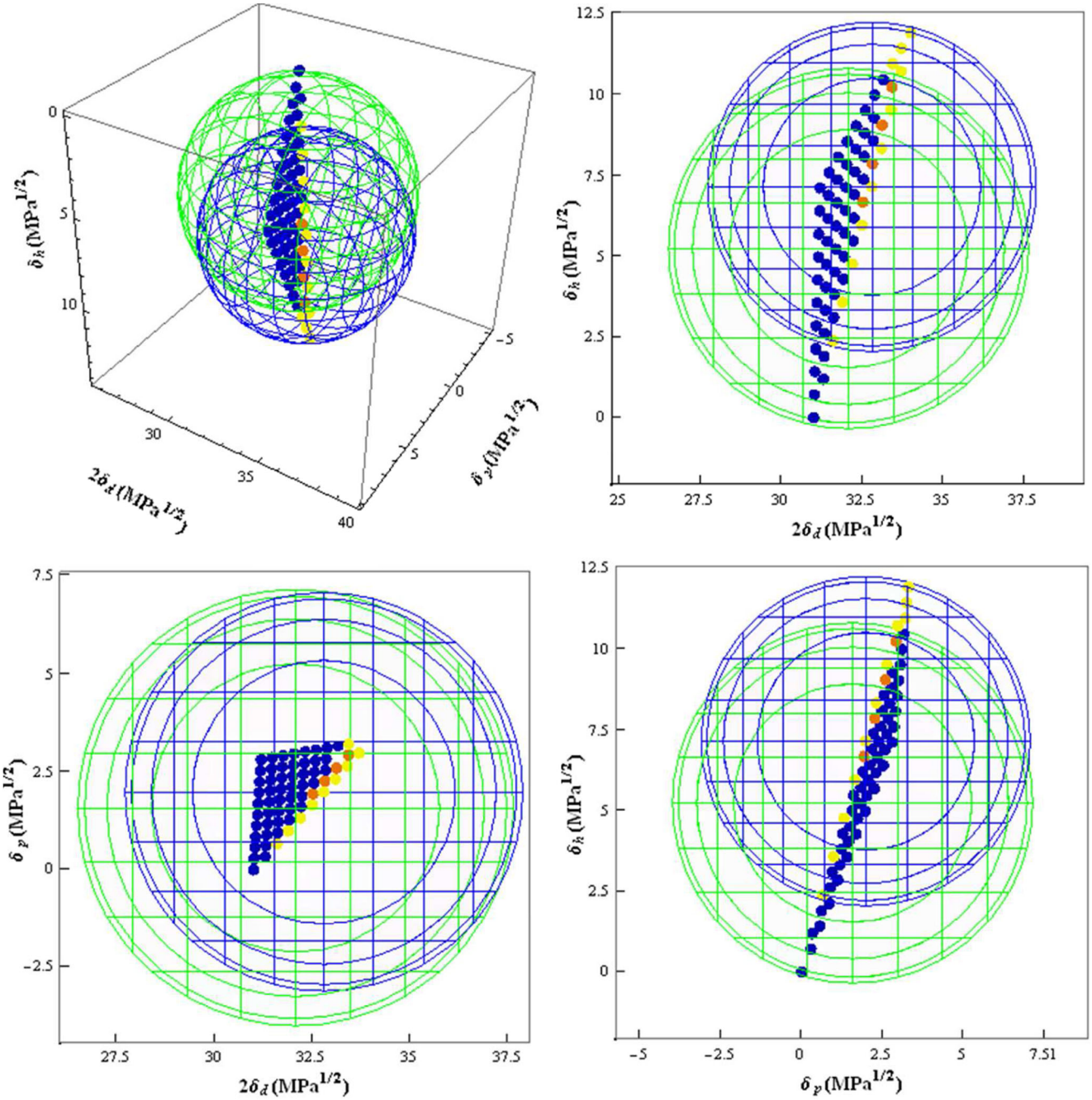

Fig. 1 2D and 3D Hansen space for the different gel, solution, and precipitate states of 12HSA/solvent combinations (i.e., octane, 1-octanol, and 1-octylamine). *Yellow points* represent solutions, *blue points* represent gels, and *orange points* represent precipitates. The *blue mesh sphere* corresponds to the solutions HSP and the *green mesh sphere* to the gel HSP

solvent combinations clustered in different regions (Fig. 1). Each of the pure solvents have similar dispersive components (i.e., $\delta_{\text{d Octane}}$=15.5 MPa$^{1/2}$, $\delta_{\text{d Octanol}}$=17.0 MPa$^{1/2}$, $\delta_{p\text{Octylamine}}$=15.6 MPa$^{1/2}$); therefore, it appears as though the points align within the spheres on the Hansen plot (Fig. 1). 12HSA precipitates occupied the smallest region of Hansen space, while the gel and solution spheres were similar in size but not location. The center ($2\delta_d$, δ_p, δ_h) of precipitate sphere is 31.7, 3.5, 8.4 MPa$^{1/2}$, and the radius (R_{pre}) is 1.94 MPa$^{1/2}$; the center of solution sphere is 31.6, 3.0, and 7.14 MPa$^{1/2}$ and the radius (R_{sol}) is 5.18 MPa$^{1/2}$. Finally, the center of gel sphere is 31.4, 2.2, and 5.23 MPa$^{1/2}$ with a radius (R_{gel}) of 5.67 MPa$^{1/2}$. However, with this system of solvent, the 3D Hansen space is unable to discern the different sols, gels, and precipitates. Thus, we were interested to study if there are any correlations with individual HSPs.

The HSPs for 12HSA, calculated using the group contribution method (δ_d=17.59 MPa$^{1/2}$, δ_p=2.86 MPa$^{1/2}$, δ_h=6.77 MPa$^{1/2}$ [13]), was used to calculate the distance between 12HSA and the solvent combinations, in Hansen space and were plotted versus the total HSP (δ_t) (Fig. 2a). It is important to note that other methods may be advantageous over determined Hansen coordinates for 12HSA including the center of the solubility sphere [27]. Bonnet et al., [27] showed that the values for 12HSA, determined using the center of the solubility sphere, differed from the group contribution methods. For R_{ij} calculations, the 12HSA coordinates were calculated using the group contribution mentions (A, C) and the center of the solubility sphere from previous works (B, D) [27]. The vector distance (R_{ij}) was calculated using Eq. 2:

$$R_{ij} = \left(4\left(_{di}-_{dj}\right)^2 + \left(_{pi}-_{pj}\right)^2 + \left(_{hi}-_{hj}\right)^2\right)^{1/2} \quad (2)$$

Below $\delta_t \sim 18.0$ MPa$^{1/2}$ gels formed at lower δ_t irrespective of the distance between the solvent and gelator and sols remained at higher δ_t (i.e., the solutions are located on the right side of the distributed data, while gels are concentrated on the left side) (Fig. 2a, b). When δ_t<18.0 MPa$^{1/2}$, no precipitates formed. Above a total HSP of 18.0 MPa$^{1/2}$, the solutions tended to lie on the right side of the data and the sols were not differentiated, in δ_t, from the precipitates (Fig. 2a). This explains why R_{ij} is not the only factor in predicting gel behavior and is unable to define clear trends between CGC and R_{ij} (Fig. 2c, d) [13]. The total HSP, related to the directionality in Hansen space, is crucial in determining organogel formation due to the fact that a strong hydrogen-bonding component or polar component may interfere with gelator-gelator interactions resulting in solutions or precipitates.

In order to better typify the gelation behavior of 12HSA in complex solvent mixtures, the CGC was assessed as a function of each individual HSP and the total HSP (Fig. 3). Solvent mixtures that contained a majority of octanol (i.e., above 50 wt%) (i.e., Fig. 3, red square) correspond to the highest CGC values. Previously, it has been shown that 12HSA in 1-octanol remains a solution; [13] therefore, the octanol-rich (octanol ≥ 50 %) solvent mixtures tend to require higher concentrations of 12HSA due to the strong gelator-solvent interaction. Even though 1-octylamine is capable of hydrogen bonding, the relative strength is lower than 1-octanol and is insufficient to impede fibrillar growth of 12HSA. Therefore, the 1-octylamine-rich gels (i.e., Fig. 3, green diamonds) correspond with lower CGC compared with 1-octanol-rich gels (red square). Furthermore, the capacity to donate and accept a hydrogen bond is very different between these two solvents. HSPiP software dissects the δ_h into the energy associated with a hydrogen bond donor and acceptor. In the case of 1-octanol, the hydrogen bond donor energy versus acceptor ratio ($\delta_{h\ D/A}$) is 6.9/8.7; for 1-octylamine, the $\delta_{h\ D/A}$ is 0.1/7.4. Since these solvents have similar energies associated with the acceptance of hydrogen bonds, the solvation of 12HSA in 1-octanol is probably due, in part, to the high hydrogen bond

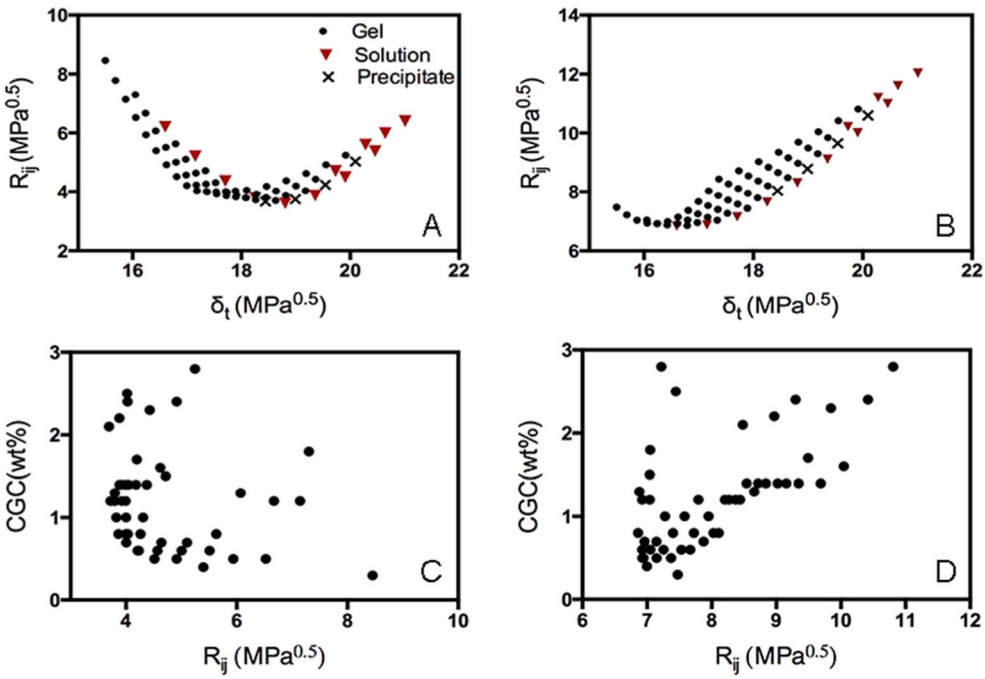

Fig. 2 The distance, in Hansen space, between 12HSA, calculated using the group contributions method (**a**, **c**) and the center of the solubility sphere (**b**, **d**) [27] and the mixed solvent systems versus the total Hansen solubility parameter (**a**, **c**) and the CGC as a function of the Hansen distance between the mixed solvents and 12HSA (**b**, **d**)

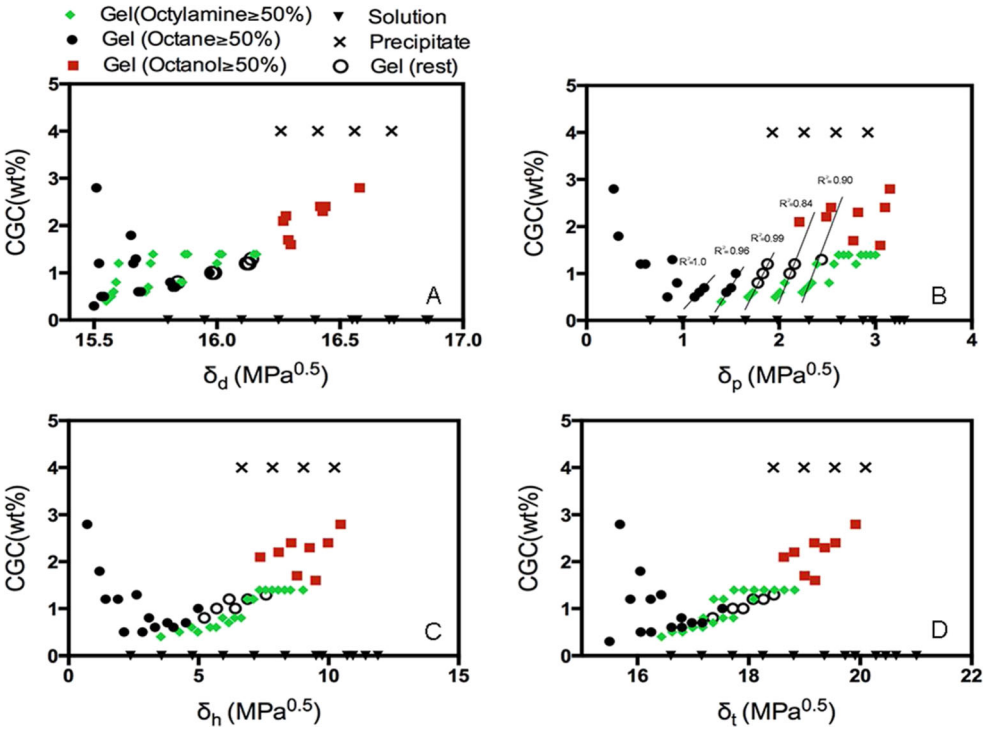

Fig. 3 CGC versus the dispersive component of the HSP (**a**), the polar component of the HSP (**b**), the hydrogen-bonding component of the HSP (**c**), and the total HSP (**d**). Precipitates are graphically illustrated arbitrarily at 4 wt% and solution are represented at 0 wt%

donating energy. Interestingly, several gels rich in octane (octane≥50 %) also correspond with high CGC. For example, the gel with 90 % of octane and 10 % of 1-octylamine has a CGC of 2.8 wt% while the CGC of pure octane is only 0.3 wt%. The vast change of CGC shows that small amounts of polar and hydrogen-bonding solvents are capable of disrupting the 12HSA fiber growth. Overall, there is no clear isolation among gel, solution, and precipitate according to the HSP. However, all of the solutions and precipitates are rich in 1-octanol (≥ 50 %) with the exception of three that are solutions rich in 1-octane (≥50 %).

Certain regions within δ_p show linear correlations with CGC. Within each region, where linearity is observed, has the same proportion of octane and varying ratios of both 1-octanol and 1-octylamine (i.e., region 1, 60 % octane, ($1.12<\delta_p<1.22$ MPa$^{1/2}$); region 2, 50 % octane ($1.4<\delta_p<1.55$ MPa$^{1/2}$); region 3, 40 % octane ($1.68<\delta_p<1.88$ MPa$^{1/2}$), region 4, 30 % octane ($1.96<\delta_p<2.16$ MPa$^{1/2}$); and region 5, 20 % octane ($2.24<\delta_p<2.54$ MPa$^{1/2}$)). As δ_p increases within each region, CGC increases with an increasing proportion of 1-octanol and a decreasing proportion of 1-octylamine (Fig. 3b). A meticulous balance between gelator-gelator interactions and gelator-solvent interactions is obtained when δ_p=1.4 MPa$^{1/2}$, δ_h=3.55 MPa$^{1/2}$ (octane=50 %, octylamine=50 %) which requires CGC<0.4 wt%. As the concentration moves away from this ratio, more gelator is required to gel the solvent mixtures. This trend becomes more evident when the data is plotted onto a ternary contour plot (Fig. 4). The CGC gradually increases as the proportion of 1-octanol increases (i.e., shown with a color change from purple to red).

The rheological behavior of 12HSA/mixed solvent gels is also quantified in terms of the HSPs, which are correlated with storage modulus (G′) (Fig. 5) and yield stress/breaking point (Fig. 6). The yield stress was experimentally defined as the stress where G′ deviates by 10 % from the average G′ obtained within the LVR. Gels rich in 1-octanol correlated to lower G′ and yield stresses compared with octane-rich or 1-octylamine-

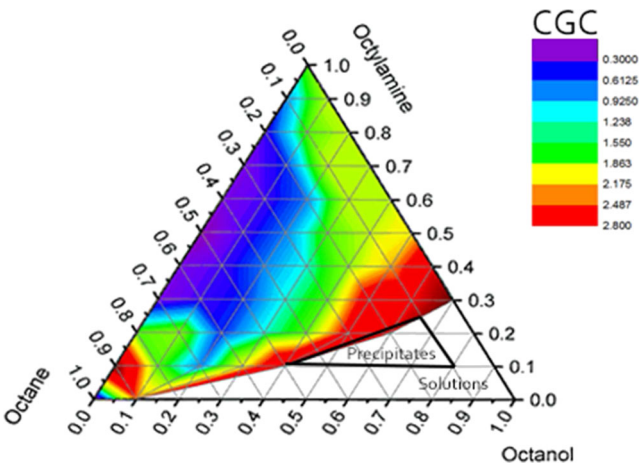

Fig. 4 2D ternary contour plot of solvents mixture systems. *Blank area* represents solutions and precipitates. *Color scale* represents the critical gelator concentration

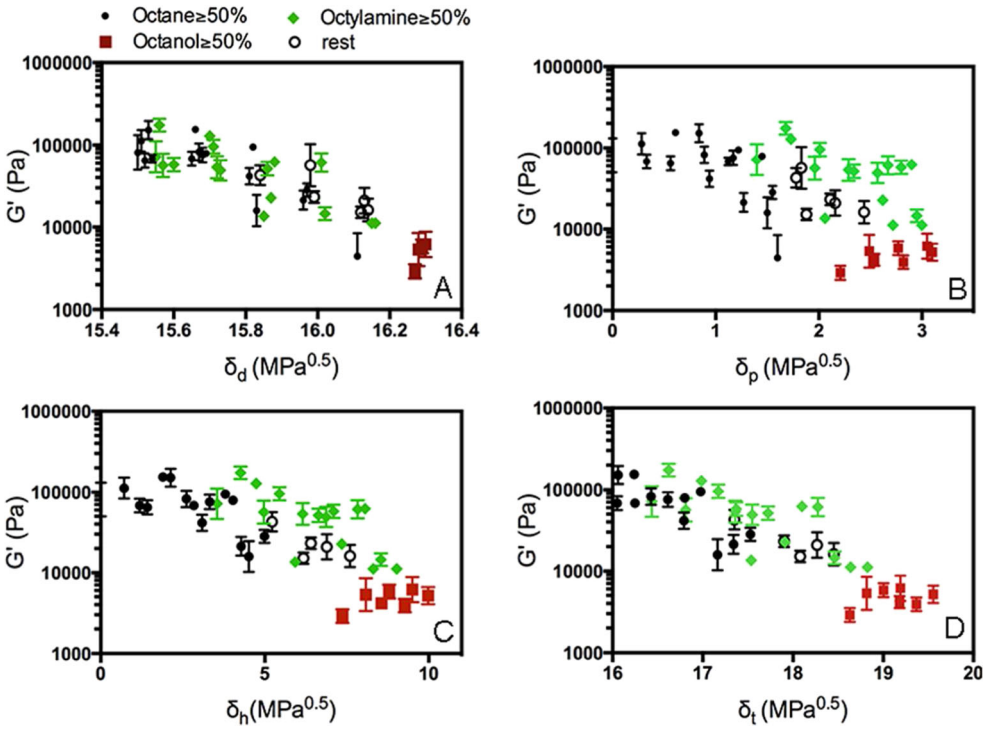

Fig. 5 Storage modulus (G′) versus the dispersive component of the HSP (**a**), the polar component of the HSP (**b**), the hydrogen-bonding component of the HSP (**c**), and the total HSP (**d**)

rich solvents. This matches with the previous findings that 12HSA in 1-octanol remains a solution and the gels rich in 1-octanol correspond with high CGC [13]. As each individual HSP or total HSP increases, both G′ and breaking points decrease in a log-linear fashion, suggesting that 1-octanol-rich gels do not form strong gels because of hydrogen bonding between 1-octanol and 12HSA which impedes fiber growth .

To further probe the effects of mixed solvents on gelation ability of 12HSA, the onset temperature of melting, as a function of each individual HSP, total HSP and CGC, was plotted (Fig. 7). There are no obvious trends found between melting temperature and solubility parameters nor between melting temperature and CGC. 12HSA in pure octane is not represented on these figures because it skews the axis as it is

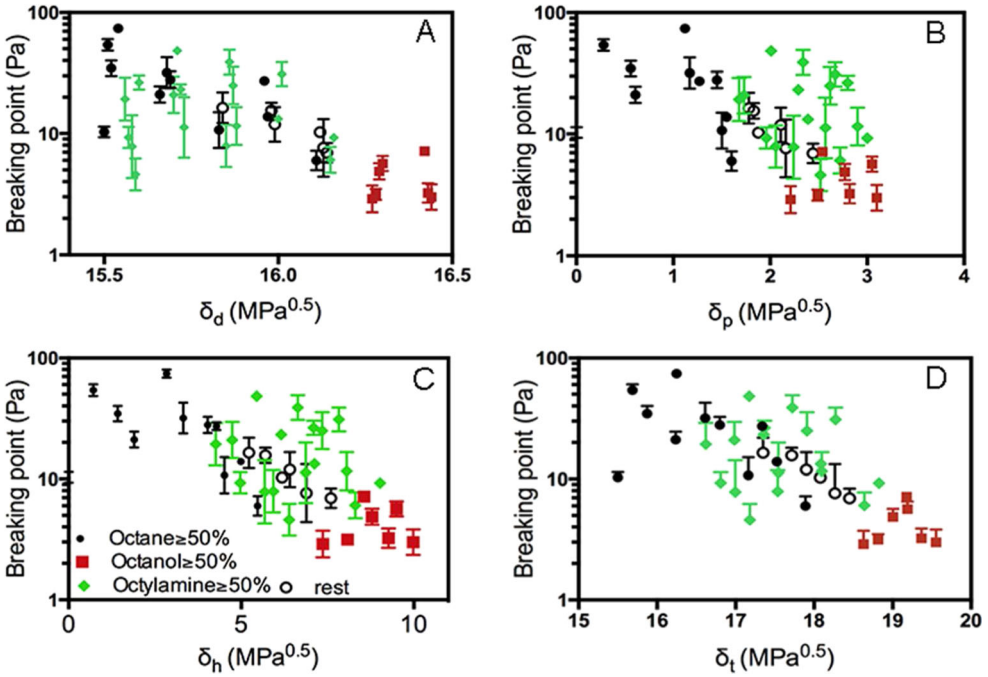

Fig. 6 Breaking point versus the dispersive component of the HSP (**a**), the polar component of the HSP (**b**), the hydrogen-bonding component of the HSP (**c**), and the total HSP (**d**)

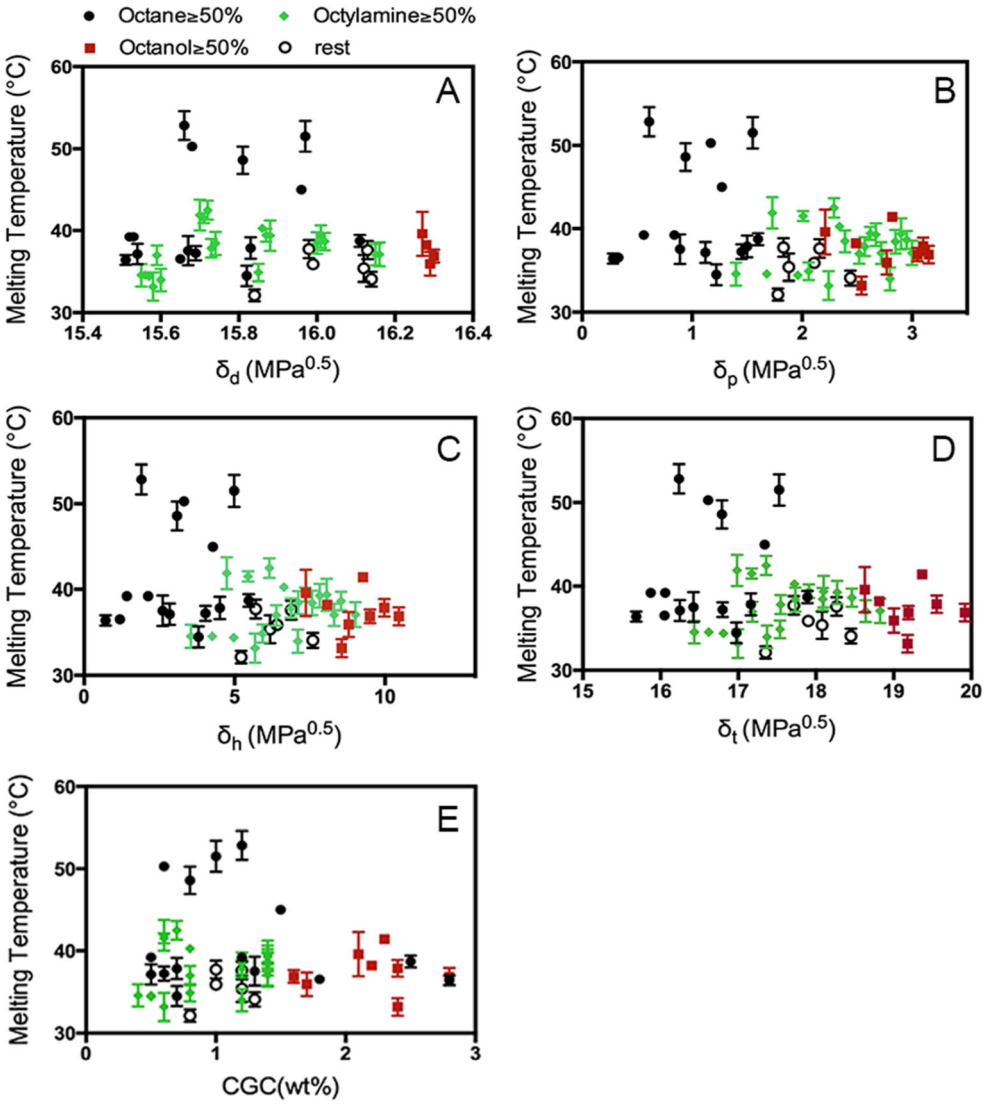

Fig. 7 Melting temperature as a function of the dispersive component δ_d (**a**), the polar component δ_p (**b**), the hydrogen-bonding component δ_h (**c**), the total HSP δ_t (**d**), and the CGC (E)

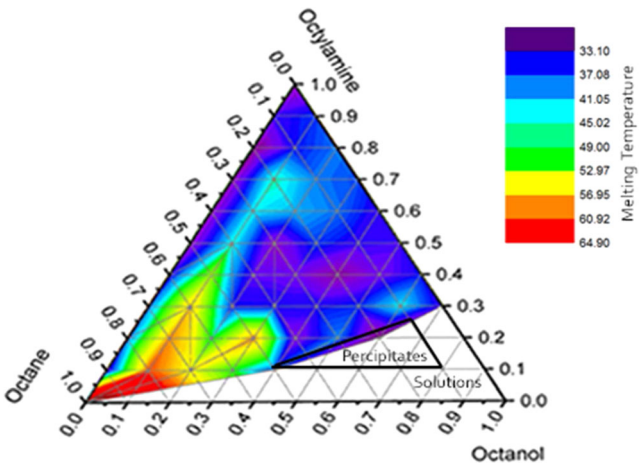

Fig. 8 2D ternary contour plot of solvents mixture concentration. *Blank area* represents solutions and precipitates

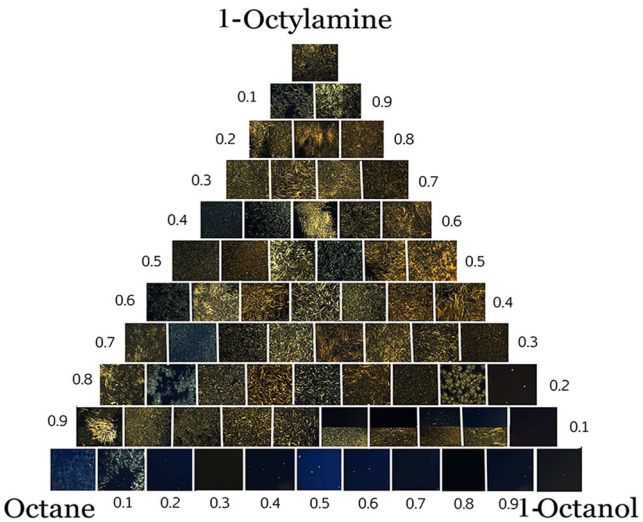

Fig. 9 Polarized light micrographs of the 12HSA organogels, precipitates, and solutions at each proportion of mixed solvents

the only system that melts above 60 °*C*. However, the five data points that have a melting temperature above 45 °*C* all have octane concentration equal to, or greater than the concentration of both 1-octanol and 1-octylamine.

It is obvious that the melting temperature drops significantly when the solvent changes from a pure octane to a solvent mixture (Fig. 8). When octane was blended with 1-octanol and/or 1-octylamine, the melting temperature dropped to between 52.83 and 32.12 °C indicating that the crystal size is decreased and/or that more imperfect crystals are present, which associated with an increase in the surface area of the crystalline structure of the molecular gel [1]. This can be explained by using Gibbs free-energy curves [40].

For the samples that remained as solutions, no fibers or spherulites were found, only a few small aggregates (Fig. 9 bottom right). The macroscopic precipitates are visually represented with images from the supernatant and precipitate as shown in the lower right side of Fig. 9. It is obvious that the morphology of the samples vary with changing solvent blends, which accounts for the changes in melting temperature. When 90 % octane was mixed with 10 % 1-octylamine, large aggregates of thick fibers were formed. As the 1-octylamine ratio increased from 10 to 50 % ($15.69 \leq \delta_t \leq 16.44$ MPa$^{1/2}$), the size of the aggregates decreased and the number of the aggregates increased. Beyond 50 % 1-octylamine ($16.63 \leq \delta_t \leq 17.37$ MPa$^{1/2}$), the size of aggregates increased resulting in thick fibers. This result correlates with observations made in the changes to the CGC. At low CGC, the crystal morphology maintains large aspect ratio with thin fibers. In binary mixtures of 1-octanol and octane, at 10 % 1-octanol, large aggregates were formed. Beyond 10 % 1-octanol ($16.6 \leq \delta_t \leq 21.01$ MPa$^{1/2}$) in the binary mixtures solutions formed. This again proved that the interaction between 12HSA and 1-octanol is more disruptive to fiber growth than 1-octylamine which may arise because of the solvents ability to accept or donate a hydrogen bond.

In this work, HSPs have been used to explain the changes observed in CGC and melting temperatures using thermodynamic arguments based on the crystal size and crystal perfection. These factors clearly play a role in the mechanism of self-assembly; however, it is important to note that this is not an exhaustive thermodynamic argument. For example, several studies have shown that addition of polar solvent, in our case 1-octanol and 1-octylamine compared to octane, will shift the phase diagram and the liquidus line of the gel between the gelator and solvent [41, 42]. Theoretically, this shift in the liquidus line will have significant effects on the solubility and hence CGC as well as the melting temperature.

Conclusion

The idea of designing this experiment on a mixed ternary solvent system provides a better understanding of the solvents effects on the 12HSA gel. Gels rich in 1-octanol (≥50 %) tend to have a higher CGC compared to gels rich in 1-octylamine (≥50 %) and gels rich in octane (≥50 %) due to the strong gelator-solvent interaction. It is clear that the hydrogen-bonding interaction (i.e., donor versus acceptor) is crucial in determining the 12HSA gel formation. Even though 1-octylamine is capable of hydrogen bonding, it is less effective in impeding fibrillar growth of 12HSA than 1-octanol. 1-Octanol-rich gels do not form strong gels because of hydrogen bonding between the gelator and solvent which impedes fiber growth.

Author contributions The manuscript was written through contributions of all authors. All authors have given approval to the final version of the manuscript.

References

1. Gao J, Wu S, Emge TJ, Rogers MA (2013) Nanoscale and microscale structural changes alter the critical gelator concentration of self-assembled fibrillar networks. CrystEngComm 15(22):4507–4515
2. Mallia VA, Butler PD, Sarkar B, Holman KT, Weiss RG (2011) Reversible phase transitions within self-assembled fibrillar networks of (R)-18-(n-Alkylamino)octadecan-7-ols in their carbon tetrachloride gels. J Am Chem Soc 133(38):15045–15054
3. Terech P, Weiss RG (2006) Introduction, in molecular gels: materials with self-assembled fibrillar networks. Springer, Dordrecht, pp 1–13
4. Li J-L, Liu X-Y, Wang R-Y, Xiong J-Y (2005) Architecture of a biocompatible supramolecular material by supersaturation-driven fabrication of its fiber network. J Phys Chem B 109(51):24231–24235
5. Rogers MA, Bot A, Lam RSH, Pedersen T, May T (2010) Multicomponent hollow tubules formed using phytosterol and γ-oryzanol-based compounds: an understanding of their molecular embrace. J Phys Chem A 114(32):8278–8285
6. Kuwahara T (1996) Crystal structure of DL-12-hydroxystearic acid. Chem Lett 25:435–436
7. Lam R, Quaroni L, Pedersen T, Rogers MA (2010) A molecular insight into the nature of crystallographic mismatches in self-assembled fibrillar networks under non-isothermal crystallization conditions. Soft Matter 6(2):404–408
8. Moffat, J. R.; Smith, D. K., Controlled self-sorting in the assembly of 'multi-gelator' gels. Chem Commun (Camb) 2009, (3), 316–8
9. Brotin TD, Fages JPF (1992) Photostationary fluorescence emission and time resolved spectroscopy of symmetrically disubstituted anthracenes on the meso and side rings: the unusual behavior of the 1,4 derivative. Photochem Photobiol 55:349–358
10. Terech P, Furman I, Weiss RG (1995) Structures of organogels based upon cholesteryl 4-(2-Anthryloxy)butanoate, a highly efficient luminescing gelator: neutron and X-ray small-angle scattering investigations. J Phys Chem 99(23):9558–9566
11. Toro-Vazquez JF, Morales-Rueda J, Mallia VA, Weiss RG (2010) Relationship between molecular structure and thermo-mechanical properties of candelilla wax and amides derived from (R)-12-

hydroxystearic acid as gelators of safflower oil. Food Biophys 5(3): 193–202
12. Wu Y, Wu S, Zou G, Zhang Q (2011) Solvent effects on structure, photoresponse and speed of gelation of a dicholesterol-linked azobenzene organogel. Soft Matter 7(19):9177–9183
13. Gao J, Wu S, Rogers MA (2012) Harnessing Hansen solubility parameters to predict organogel formation. J Mater Chem 22(25): 12651–12658
14. Kubo W, T KM, Kitamura S, Yodhida M, Haruki K, Hanabusa H, Shirai Y, Wada, Yanagida S (2011) Quasi-solid- state dye-sensitized TiO2 solar cells: effective charge transport in mesoporous space filled with gel electrolytes containing iodide and iodine. Phys Chem B 105: 12809–12815
15. Sugiyasu K, a Ss NF (2004) Visible-light-harvesting organogel composed of cholesterol-based perylene derivatives. Chem Int Ed 43: 1229–1233
16. Friggeri A, Feringa BL, van Esch J (2004) Entrapment and release of quinoline derivatives using a hydrogel of a low molecular weight gelator. ContrL Rel 97:241–248
17. Marangoni A (2012) Organogels: an alternative edible oil-structuring method. J Am Oil Chem Soc 89(5):749–780
18. Raynal M, Bouteiller L (2011) Organogel formation rationalized by Hansen solubility parameters. Chem Commun 47(29):8271–8273
19. Fan K, Niu L, Li J, Feng R, Qu R, Liu T, Song J (2013) Application of solubility theory in bi-component hydrogels of melamine with di(2-ethylhexyl) phosphoric acid. Soft Matter 9(11):3057–3062
20. Niu L, Song J, Li J, Tao N, Lu M, Fan K (2013) Solvent effects on the gelation performance of melamine and 2-ethylhexylphosphoric acid mono-2-ethylhexyl ester in water-organic mixtures. Soft Matter 9(32):7780–7786
21. Bielejewski M, Łapiński A, Luboradzki R, Tritt-Goc J (2009) Solvent effect on 1,2-O-(1-ethylpropylidene)-α-d-glucofuranose organogel properties. Langmuir 25(14):8274–8279
22. Zhu P, Yan X, Su Y, Yang Y, Li J (2010) Solvent-induced structural transition of self-assembled dipeptide: from organogels to microcrystals. Chemistry 16(10):3176–3183
23. Kaszyńska J, Łapiński A, Bielejewski M, Luboradzki R, Tritt-Goc J (2012) On the relation between the solvent parameters and the physical properties of methyl-4,6-O-benzylidene-α-d-glucopyranoside organogels. Tetrahedron 68(20):3803–3810
24. Wu S, Gao J, Emge TJ, Rogers MA (2013) Solvent-induced polymorphic nanoscale transitions for 12-hydroxyoctadecanoic acid molecular gels. Cryst Growth Des 13(3):1360–1366
25. Wu S, Gao J, Emge TJ, Rogers MA (2013) Influence of solvent on the supramolecular architectures in molecular gels. Soft Matter 9(25): 5942–5950
26. Hirst AR, Smith DK, Feiters MC, Geurts HP (2004) Two-component dendritic gel: effect of stereochemistry on the supramolecular chiral assembly. Chemistry 10(23):5901–5910
27. Bonnet J, Suissa G, Raynal M, Bouteiller L (2014) Organogel formation rationalized by Hansen solubility parameters: dos and don'ts. Soft Matter 10(18):3154–3160
28. Curcio P, Allix F, Pickaert G, Jamart-Grégoire B (2011) A favorable, narrow, δh Hansen-parameter domain for gelation of low-molecular-weight amino acid derivatives. Chem Eur J 17(48):13603–13612
29. Yan Ni, N.; Xu Zhiyan, Z.; Diehn Kevin, K. K.; Raghavan Srinivasa, R. S.; Fang Yu, Y.; Weiss Richard, G. R., 2013; Vol. 135, p 8989–99
30. Yan N, Xu Z, Diehn KK, Raghavan SR, Fang Y, Weiss RG (2013) How do liquid mixtures solubilize insoluble gelators? Self-assembly properties of pyrenyl-linker-glucono gelators in tetrahydrofuran—water mixtures. J Am Chem Soc 135(24):8989–8999
31. Tong C, Fan K, Niu L, Li J, Guan X, Tao N, Shen H, Song J (2014) Application of solubility parameters in a d-sorbitol-based organogel in binary organic mixtures. Soft Matter 10(5):767–772
32. Shen H, Niu L, Fan K, Li J, Guan X, Song J (2014) Application of solubility parameters in 1,3:2,4-Bis(3,4-dimethylbenzylidene)sorbitol organogel in binary organic mixtures. Langmuir 30(30):9176–9182
33. Diehn KK, Oh H, Hashemipour R, Weiss RG, Raghavan SR (2014) Insights into organogelation and its kinetics from Hansen solubility parameters. Toward a priori predictions of molecular gelation. Soft Matter 10(15):2632–2640
34. Lan, Y.; Corradini, M. G.; Liu, X.; May, T. E.; Borondics, F.; Weiss, R. G.; Rogers, M. A. (2014) Comparing and correlating solubility parameters governing the self-assembly of molecular gels using 1,3: 2,4-dibenzylidene sorbitol as the gelator. Langmuir
35. Abdala AA, Olesen K, Khan SA (2003) Solution rheology of hydrophobically modified associative polymers: solvent quality and hydrophobic interactions. J Rheol 47(2):497
36. E. A. Grulke, J. W. S. N. Y. (2005) Solubility parameter values. NewYork (4th edn)
37. Jang M, Kamens RM, Leach KB, Strommen MR (1997) A thermodynamic approach using group contribution methods to model the partitioning of semivolatile organic compounds on atmospheric particulate matter. Environ Sci Technol 31:2805–2811
38. Fedors RF (1974) A method for estimating both the solubility parameters and molar volumes of liquids. Polym Eng Sci 14:147–154
39. Lindvig T, Michelsen ML, Kontogeorgis GM (2002) A Flory–Huggins model based on the Hansen solubility parameters. Fluid Phase Equilib 203(1–2):247–260
40. Fabri D, Guan J, Cesàro A (1998) Crystallisation and melting behaviour of poly (3-hydroxybutyrate) in dilute solution: towards an understanding of physical gels. Thermochim Acta 321(1–2):3–16
41. Feng L, Cavicchi KA (2012) Investigation of the relationships between the thermodynamic phase behavior and gelation behavior of a series of tripodal trisamide compounds. Soft Matter 8(24):6483–6492
42. Hirst AR, Coates IA, Boucheteau TR, Miravet JF, Escuder B, Castelletto V, Hamley IW, Smith DK (2008) Low-molecular-weight gelators: elucidating the principles of gelation based on gelator solubility and a cooperative self-assembly model. J Am Chem Soc 130(28):9113–9121